



**HAL**  
open science

## Losses estimation method by simulation for the Modular Multilevel Converter

Julian Freytes, François Gruson, Philippe Delarue, Frédéric Colas, Xavier Guillaud

► **To cite this version:**

Julian Freytes, François Gruson, Philippe Delarue, Frédéric Colas, Xavier Guillaud. Losses estimation method by simulation for the Modular Multilevel Converter. EPEC2015, Oct 2015, London, United Kingdom. pp.00. hal-03170506

**HAL Id: hal-03170506**

**<https://hal.science/hal-03170506v1>**

Submitted on 16 Mar 2021

**HAL** is a multi-disciplinary open access archive for the deposit and dissemination of scientific research documents, whether they are published or not. The documents may come from teaching and research institutions in France or abroad, or from public or private research centers.

L'archive ouverte pluridisciplinaire **HAL**, est destinée au dépôt et à la diffusion de documents scientifiques de niveau recherche, publiés ou non, émanant des établissements d'enseignement et de recherche français ou étrangers, des laboratoires publics ou privés.

# Losses Estimation Method by Simulation for the Modular Multilevel Converter

Julian Freytes, François Gruson, Philippe Delarue, Frederic Colas, Xavier Guillaud  
Laboratoire d'Electrotechnique et Electronique de Puissance (L2EP)  
Lille, France

**Abstract**—The modular multilevel converter (MMC) is the most promising solution to connect HVDC grids to an HVAC one. The installation of new equipment in the HVDC transmission systems requires an economic study where the power losses play an important role. Since the MMC is composed of a high number of semiconductor elements, the losses estimation becomes complex. This paper proposes a simulation-based method for the losses estimation that combines the MMC averaged and instantaneous model in a modular way. The method brings the possibility to compare performances for different modules technologies as well as different high and low level control techniques. The losses characteristics within the MMC are also discussed. The passive losses are taken into account for the first time.

**Index Terms**—Conduction losses, Modular Multilevel Converter (MMC), passive losses, switching losses.

## I. INTRODUCTION

The great advances in power electronics and its control allowed considering the high voltage DC transmission systems (HVDC) as a viable solution. One of the most promising converters for HVDC systems is the Modular Multilevel Converter, which is a three phase VSC that was first introduced in [1]. The main advantage respect to the classical VSCs is the possibility of working with a low switching frequency while achieving at the same time lower losses and better performances [2]. The main drawback is the high number of components that leads to very complex models and control system. The control of this converter was largely discussed on the literature in the last decade but the losses estimation was less studied [3][4][5].

The installation of new equipment in the transmission systems requires an economic study where the power losses play an important role [2]. But it is also important to have a comparative tool for different aspects in terms of losses since it is not trivial to obtain experimental results with high power rating converters [6].

There are three main methods for estimating the power losses in the MMC. The first one is a complete analytic approach where the currents and voltages waveforms and the switching functions for the submodules can be expressed in an analytic form [2][7]. The main advantage is the low

computing time, but the main drawback is the difficulty for estimating the switching losses. Also it is not easily adaptive for taking into account different control techniques [5]. The second method is based on the MMC simulation using the analytic expressions of the voltages and currents as model inputs for deducing the switching behavior of the submodules. This method is not as fast as the analytical one but the switching functions of the submodules are obtained more accurately and so the switching losses are more precisely estimated. As previously discussed, different high level control methods are not easily considered either. The third method is a numerical approach that consists in the simulation of the entire MMC and its control system. The losses can be calculated as a direct result from the simulation [8]. If a high number of submodules is considered, an extremely high computational effort would be necessary to achieve it. Simulating a MMC with 400 submodules per arm, for a certain number of power cycles, it takes up to ten minutes [9].

The proposed method in this paper is based on two consecutive simulations. The first one considers the averaged model of the converter where different High Level Control techniques can be applied. The results of these simulations are used as inputs for a second simulation that considers a complete MMC arm with its Low Level Control. Ideal switches are considered at this step. With the results obtained from both simulations the losses are calculated with a script where different modules technologies can be studied. With this method it is possible to compare in term of losses different High Level Control and Low Level Control techniques and parameters (such as amount of submodules or control switching frequency) and also different IGBT technologies. It presents the advantage of being more adaptive for different control strategies with a small computation time.

This paper is organized as follows. Section II recalls the MMC structure and the control hierarchy. Section III presents a MMC losses description. The proposed losses estimation method is presented in Section IV. In Section V it is showed the simulation results and the analysis of the losses in the MMC. Conclusions are stated in Section VI.

## II. MMC GENERALITIES AND DEFINITIONS

### A. MMC Topology

Fig. 1 shows the topology of a three phase Modular Multilevel Converter. It has three legs that form each of the phases and each leg has two arms (upper and lower arm).

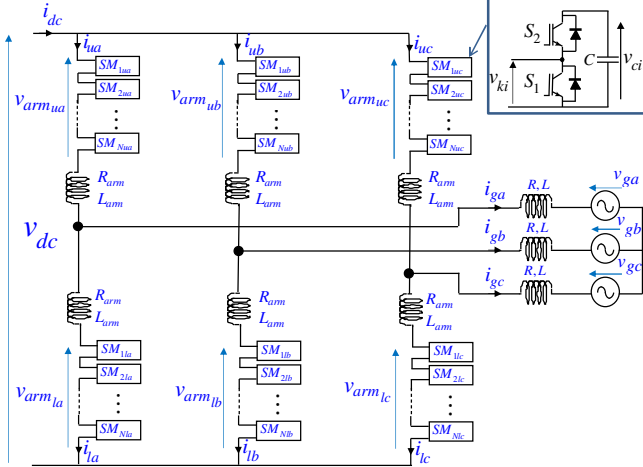


Figure 1. MMC Topology

The arms are composed by  $N$  submodules (SM) connected in series and each of them have two switches; lower switch  $S_1$  (with the IGBT  $T_1$  and diode  $D_1$ ); and upper switch  $S_2$  (with the IGBT  $T_2$  and diode  $D_2$ ), and a capacitor  $C$  whose voltage drop, for the SM  $i$ , is expressed as  $v_{Ci}$ . The number of submodules can vary depending on the application and the desired output voltage level. For a 401-Level MMC-HVDC system  $N$  is equal to 400 [9].

When the SM is enabled (switch  $S_2$  in ON-state,  $S_1$  in OFF-state) the SM output voltage  $v_{ki}$  is equal to  $v_{Ci}$  and it starts to conduct the arm current  $i_{arm}$  which will charge or discharge the SM capacitor  $C$  depending on the currents direction. When the SM is bypassed (switch  $S_2$  in OFF-state,  $S_1$  is in ON-state) the SM output voltage  $v_{ki}$  is zero and its capacitor voltage remains at the same level. The arm voltage  $v_{arm,ul_j}$  will be formed by the sum of the activated SM voltages, so the output voltage will have a discrete form with  $N+1$  levels.

The arm inductances  $L_{arm}$  reduce the internal current between the phases, limit the fault currents gradients and support the voltage difference caused by the insertion and disconnection of the submodules [1]. The inductances in the AC filter  $L_f$  correspond to the MMC output transformer. The resistive part of the arm inductances and the output filter are noted as  $R_{arm}$  and  $R_f$  respectively.

### B. Control Hierarchy

The control system structure for the MMC is presented in Fig. 2. It is composed by the *High Level Control* which will determine the six arm voltages ( $v_{arm,ref}$  for each arm among

the phases) desired to fulfill the requirements such as output power and/or DC voltage level.

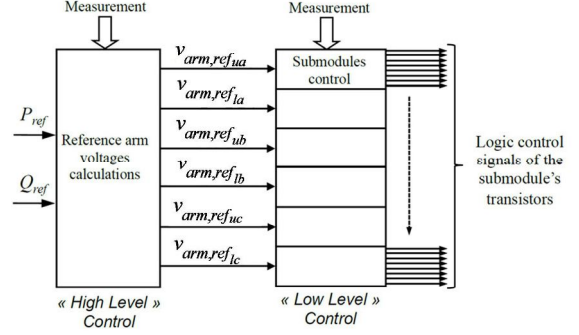


Figure 2. Control structure

The *Low Level Control* will be in charge of the transistors gate signals in order to select the amount of submodules needed to form the desired arm voltage and hence, the output AC voltage. Also it determines which submodule will be chosen in order to balance the capacitor voltages. This is done with the Balancing Control Algorithms (BCA).

## III. MMC LOSSES DESCRIPTION

The losses in the MMC can be divided into semiconductor losses (conduction and switching losses) and passive losses.

### A. Semiconductor losses

#### 1) Conduction losses

While conducting, the semiconductors have an on-state voltage drop which varies non-linearly with the current and with the junction temperature  $T_j$ . Typically noted as  $V_F(i)$  for the diodes, and  $V_{CEsat}(i)$  for the IGBTs. The module's manufacturers provide the on-state characteristics curves in their datasheets for a limited number of junction temperatures. The on-state characteristics of the module *Mitsubishi CM1500HC-66R* is showed in Fig. 3 [10]. It is also showed the linear and high order polynomial approximations.

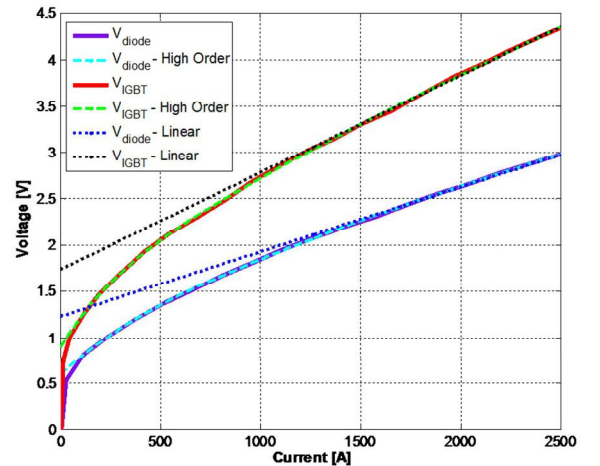


Figure 3. Collector-Emitter saturation voltage characteristics - CM1500HC66R ( $T_j=150^\circ\text{C}$ ).

When using linear approximation it is clearly observed that, for low values of current, the on-state voltage drop of the diode and IGBT is overestimated. This conduces to an overestimation of the losses.

The conduction losses in the semiconductors of a given submodule can be calculated as the product of the current  $i_{arm}$  passing across the component and its voltage drop. The conduction losses ( $p_c$ ) in the diodes and IGBTs can be calculated as showed in the equations (1) to (4), where  $f_{D1}$ ,  $f_{T1}$ ,  $f_{D2}$  and  $f_{T2}$  are Boolean functions so when the value is 1, the current is flowing through the respective element and 0 otherwise.

$$P_{c,diode D1}(t) = f_{D1} \cdot i_{arm} \cdot V_F(i_{arm}, T_j) \quad (1)$$

$$P_{c,IGBT T1}(t) = f_{T1} \cdot i_{arm} \cdot V_{CE(sat)}(i_{arm}, T_j) \quad (2)$$

$$P_{c,diode D2}(t) = f_{D2} \cdot i_{arm} \cdot V_F(i_{arm}, T_j) \quad (3)$$

$$P_{c,IGBT T2}(t) = f_{T2} \cdot i_{arm} \cdot V_{CE(sat)}(i_{arm}, T_j) \quad (4)$$

The average losses of each semiconductor element in a submodule can be calculated integrating the equations (1) to (4) over a power cycle.

The difficulty for calculating the conduction losses for each element of the MMC is that it is not trivial to find an analytical expression for  $f_{D1}$ ,  $f_{T1}$ ,  $f_{D2}$  and  $f_{T2}$  of the equations (1) to (4). In [11] it is proposed a probabilistic approach for defining a continuous function that indicates the fraction of submodules in the arm that are active as a function of time. This allows reformulating the equations (1) to (4) taking into account the complete arm and not each semiconductor device. In that method it is imperative to consider ideal BCAs, and different control algorithms are not easily taken into account. In this paper the aforementioned functions are obtained by simulation.

## 2) Switching losses

Each time a semiconductor device switches, a small amount of energy is lost. The IGBT turn on and turn off lost energies are typically denoted as  $E_{on}$  and  $E_{off}$  respectively. The energy losses due to the reverse recovery phenomena in the diode are denoted as  $E_{rec}$ .

The switching energy depends on several parameters but most importantly on the current and the junction temperature. These energies can be obtained from the manufacturer's datasheets as curves in function of  $T_j$ , the current passing through the component and the blocking voltage (usually noted as  $V_{CC}$ ). The switching energy characteristics of the module *Mitsubishi CM1500HC-66R* is shown in Fig. 4 [10]. For another blocking voltage value  $V_{CC}$ , a simple linear interpolation can be done in order to correct the lost energy.

The characteristics are also normally approximated with linear functions as for the conduction losses.

For the IGBTs, a linear interpolation could be an acceptable approximation but for the energy lost in the diodes ( $E_{rec}$ ) it is not sufficient and it will cause an overestimation of the losses. In this paper the switching energy characteristics are approximated with high order polynomial functions.

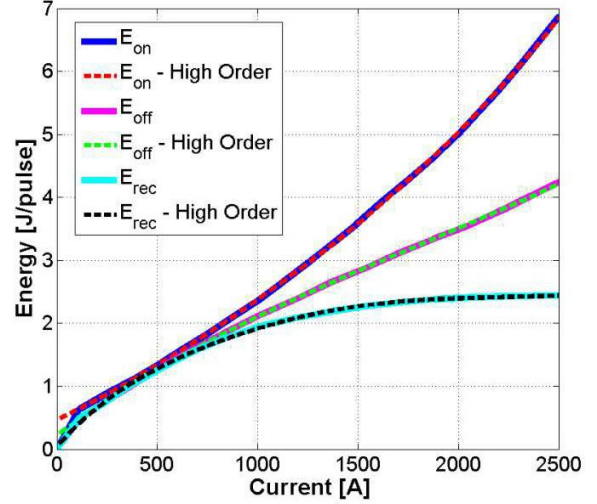


Figure 4. Half-bridge switching energy characteristics (Typical) - CM1500HC-66R ( $T_j=150^\circ\text{C}$ ,  $V_{CC}=1800\text{V}$ ).

The energy lost at each commutation event for the IGBT (turn on and turn off) and diode (turn off) are expressed in the following equations, where  $v_{Ci}$  is the submodule's capacitor voltage value at the moment of the commutation.

$$IGBT_{turn\_on} \rightarrow E_{on}(i_{arm}, T_j) \frac{v_{Ci}}{V_{CC}} \quad (5)$$

$$IGBT_{turn\_off} \rightarrow E_{off}(i_{arm}, T_j) \frac{v_{Ci}}{V_{CC}} \quad (6)$$

$$Diode_{turn\_off} \rightarrow E_{rec}(i_{arm}, T_j) \frac{v_{Ci}}{V_{CC}} \quad (7)$$

For calculating the total switching losses, the equations (5) to (7) are used at each commutation event, and the results are summed up and averaged during a fundamental period.

## B. Passive losses

The passive losses are due to the resistive part of the arm inductances  $R_{arm}$ , the AC side filter  $R_f$  and the capacitor's equivalent series resistor  $R_{ESR}$ . The losses due to the auxiliaries' components and the controller itself are not taken into account since they are relatively small compared with the total losses. Also, they are independent of the operating point of the MMC.

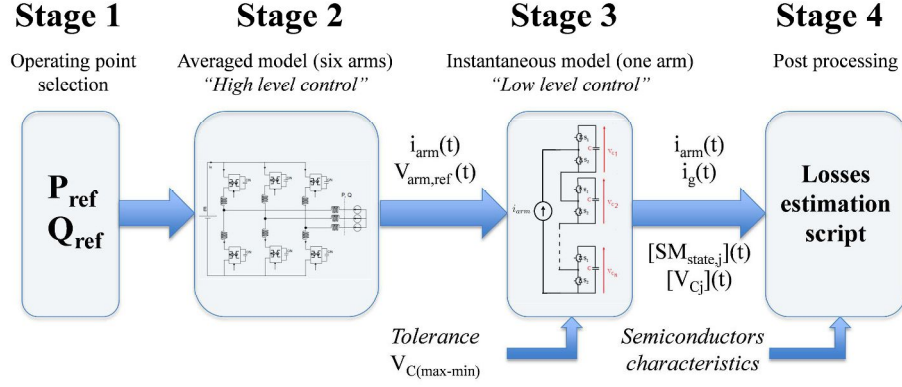


Figure 5. Schema of the proposed losses calculation method

#### IV. MMC LOSSES ESTIMATION METHOD

The proposed numerical method for estimating the losses in the MMC consists in four stages as it can be seen in Fig. 5.

##### A. Stage 1

The first step is to set up an operating point in terms of the active and reactive power;  $P_{ref}$  and  $Q_{ref}$  respectively.

##### B. Stage 2

The complete MMC averaged model with a specific control technique is simulated (i.e. *High Level Control*). It is recalled that any control strategy can be applied at this step (e.g. the control strategy proposed in [3], [4], and so on).

The model used at this stage is detailed in [12], which is based in the assumption that all the capacitors within an arm have the same instantaneous value. With this assumption an equivalent averaged model for each arm can be obtained.

The results obtained for the steady state of one arm voltage  $v_{arm}$  and current  $i_{arm}$  (outputs of the *Stage 2*) are used in the following stage as inputs.

##### C. Stage 3

At this stage only one arm is simulated since the losses will be equally distributed among the arms due to the symmetry of the converter (Fig. 7). This simplification allows reducing the total simulation time while obtaining similar results.

The arm voltage  $v_{arm}$  will be used as the reference voltage  $v_{arm,ref}$  and the arm currents  $i_{arm}$  will be implemented as a current source for the arm simulation. The arm is modeled as in [2]. The power switches are assumed as ideal ones. For following the reference voltage, any *Low Level Control* strategy can be applied (Nearest Level Control, PWM or others). Also a BCA is implemented in this stage [13]. It is defined the *tolerance* band between the most charged and less charged capacitor.

##### D. Stage 4

The post processing algorithm calculates the losses for each semiconductor (switching and conduction losses) as well

as the passive losses in the MMC based on the results of the *Stage 2*, *Stage 3* and the chosen *semiconductor characteristics*.

The algorithm is based on the information of the Fig. 6 where it can be observed four possible states for a submodule, regarding the state of the SM and the current's direction.

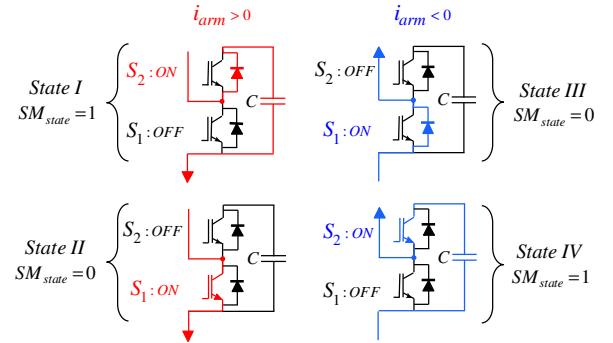


Figure 6. Arm current path in a submodule and possible cases in switching events

The conduction losses are calculated for each semiconductor component taking into account the SM state and the arm current direction. For identifying the semiconductor component of the submodule that is in conduction mode at a given moment the following evaluation is performed:

- When  $SM_{state}$  is equal to 1 and the arm current is positive, the diode  $D_1$  is in conduction mode (State I). If the current is negative, the IGBT  $T_1$  is conducting (State III). For both cases, the arm current passes through the submodules capacitor (i.e. there are instantaneous losses in the capacitor's equivalent series resistor  $R_{ESR}$ ).
- When  $SM_{state}$  is equal to 0 and the current is positive, the IGBT  $T_2$  is conducting. If the current is negative, the diode  $D_2$  is in conduction mode. In this case the capacitor voltage remains constant since the submodule is disabled.

The switching losses are also calculated for each component regarding the changes in the switching states of the

submodules ( $SM_{state} : 1 \rightarrow 0$  or  $0 \rightarrow 1$ ) and the arm current direction in order to determine which semiconductor is switched (diode or IGBT). Taking into account the Fig. 6, this is determined as follows: When the arm current is positive and the  $SM_{state}$  changes from *State I* to *State II*, the diode  $D_1$  stops conducting with an energy lost that can be calculated with Eq. (7), and the IGBT  $T_2$  turns on dissipating an energy calculated with Eq. (5). If the  $SM_{state}$  changes from *State II* to *State I*, the IGBT  $T_2$  turns off dissipating an amount of energy calculated with Eq. (6) and the diode  $D_1$  starts conducting with a lost energy that is neglected. Similar analysis can be performed when the current is negative.

The script accumulates the energy lost for one power cycle and averages it through it [2]. Since the *Stage 3* considers only one arm, the semiconductor losses are calculated for one arm and then extended to the six arms.

## V. SIMULATION RESULTS

This section shows the simulation results for a 401-Level MMC. The main parameters are listed in table I. The submodule chosen for the simulations is the *Mitsubishi CM1500HC-66R*.

TABLE I. MMC PARAMETERS

Rated Active and Reactive Power		1.1GW , 500MVar	
$N$	400	$T_j$	150°C
$C$	10mF	$R_{ESR}$	0.1mΩ
$L_{arm}$	50mH	$R_{arm}$	0.05Ω
$L_f$	60mH	$R_f$	0.06Ω

### A. MMC Losses Analysis

#### 1) Instantaneous energy lost

Fig. 7 shows the instantaneous energy lost in the six arms of the MMC. The power losses will be given by the slope of the sum of each curve. This result validates the assumption made at the *Stage 3*.

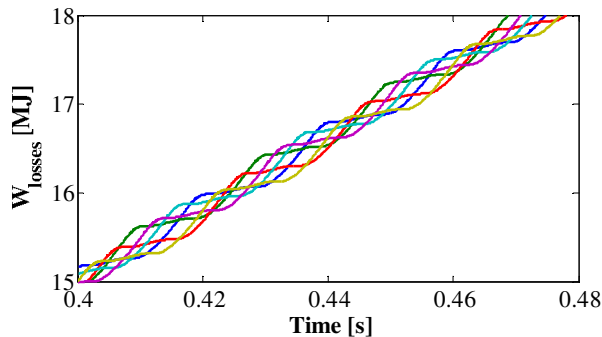


Figure 7. Instantaneous energy lost in the semiconductor elements of the six MMC arms.

#### 2) Total losses and efficiency

Fig. 8 shows the total losses for different operating points and two different junction temperatures  $T_j$  provided in the datasheet of the chosen semiconductor device. It can be

observed a non-symmetrical parabolic surface since the losses while working in rectifying mode ( $P < 0$ ) are lower than in inverting mode ( $P > 0$ ). Also, it is observed a symmetrical behavior respect to the reactive power.

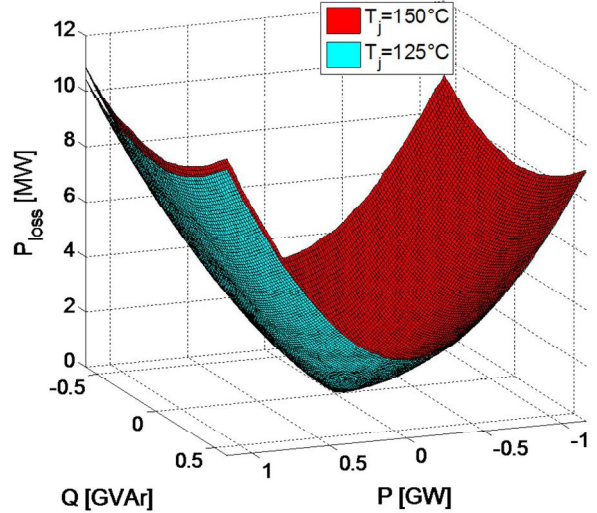


Figure 8. Total losses with *Mitsubishi CM1500HC-66R*.

As it can be seen in Fig. 8, the losses increase with the junction temperature for every operating point.

Fig. 9 shows the efficiency of the converter defined as  $Efficiency[\%] = 100 P / (P + P_{losses})$ . The junction temperature is fixed to  $T_j = 150^\circ C$ . It is clearly seen that when the reactive power consumption or production is zero the efficiency is maximal. Results from Fig. 9 show that the efficiency of the MMC is in the range of 98% to 99.5% [6].

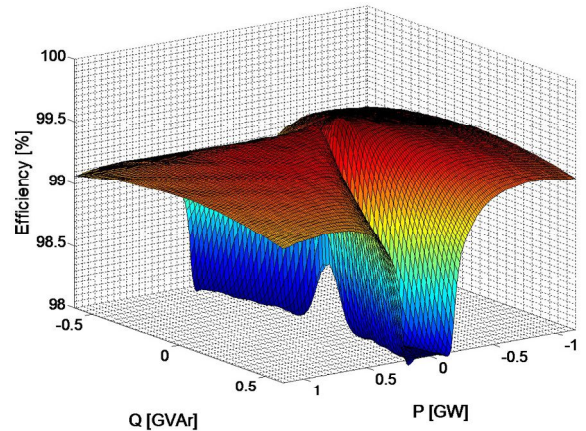


Figure 9. Efficiency of the MMC.

#### 3) Separated Losses

Fig. 10 shows the conduction, switching and passive losses where it can be observed that the conduction losses are the most important. The conduction losses are greater than the switching losses with the studied IGBT module. This is due to the new IGBT generation since they have low switching losses (but higher conduction losses); making it attractive for

classical VSC but not so suitable for MMC. In this case it would be a better option to have components with lower conduction losses (and higher switching losses). The IGBT design is always a compromise between conduction and switching losses.

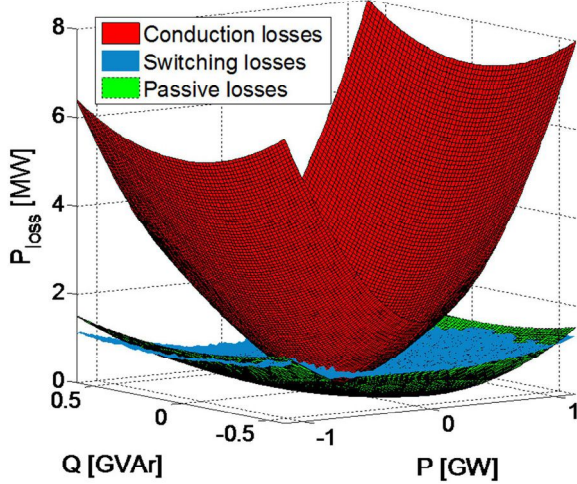


Figure 10. Separated losses: Conduction, switching and passive losses.

The passive losses are comparable to the switching losses and for high values of power transmission, the passive losses become even higher. They should be taken into account for limiting the error in the losses estimation.

#### 4) Passive losses

Fig. 11 shows the result for the different passive losses considered in this paper.

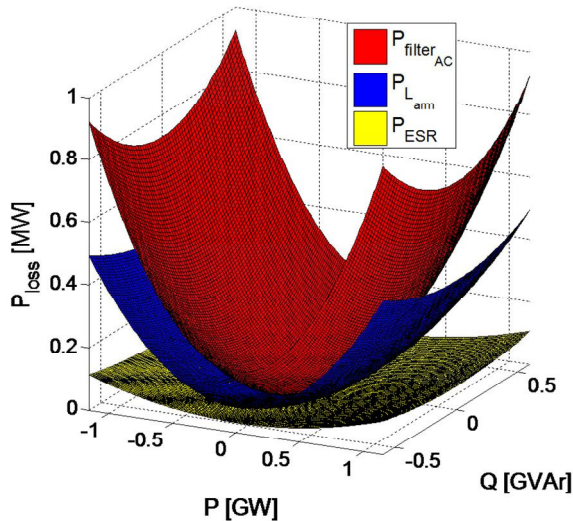


Figure 11. Passive losses. AC filter, arm inductance and equivalent series resistor losses.

The capacitor losses are less than 0.01% of the nominal power for every operating point. The losses in the AC filter are the most significant. Nevertheless, they are always less than 1MW that corresponds to less than 0.09% of the nominal

active power. The losses in the arm inductances are less than 0.045%. In [6] it is stated that, as a rule of thumb, 0.3% must be expected for the passive filters in total at nominal power. Results show that they are less than 0.135%.

### B. Losses comparisons

#### 1) Semiconductors characteristics approximation

Normally the semiconductors characteristics are approximated with linear functions. As it was stated before, this conducts to an overestimation of the losses. For computing the difference between linear and higher order approximations it is defined  $P_{linear}$  and  $P_{higher}$  as the total power losses obtained when considering the linear and higher order polynomial approximation respectively. Results are shown in Fig. 12 where  $\Delta P_{loss} = P_{linear} - P_{higher}$ .

Results of Fig. 12 show that in average the difference in the losses estimation is 150kW. Considering 10c€/kWh as the losses price, the error estimation results in 131k€/year.

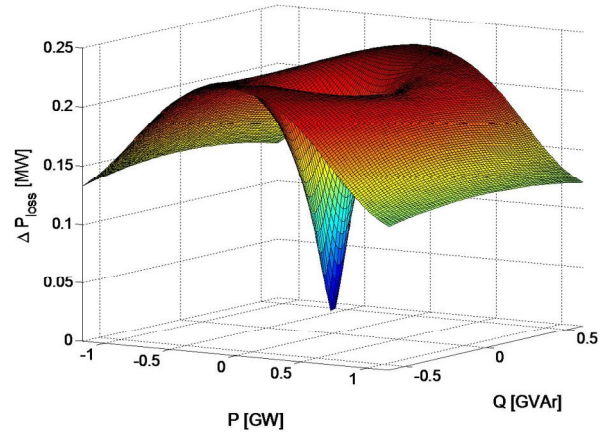


Figure 12. Losses comparison with linear and high order approximation for the semiconductors on-state characteristics.

#### 2) High Level Control options

In this part it is compared two types of control strategies in terms of power losses. Since the total stored energy level in the MMC is the result of the power difference between the AC and DC side of the MMC, in the control structure, a compensation term appears of the power in each arm by the AC phases ( $p_{ACi}$ ). It is possible to compensate either the average value of  $p_{ACi}$  or its instantaneous value.

With the use of the loss estimation method proposed in this paper it is possible to show that in some cases the usual choice is not the best one in terms of losses. This is detailed in [14] and the results are showed in Fig. 13.

#### 3) Modules comparisons

With the proposed method it is possible to evaluate different silicon switches. In this part, the modules *Mitsubishi CM1500HC-66R* and *Infineon FZ1500R33HE3* [15] are compared in terms of power losses. The power difference is defined as  $\Delta P = P_{Mitsubishi} - P_{Infineon}$ . Positive values of  $\Delta P$

corresponds to lower losses for the *Infineon* module and vice versa. The results are showed in Fig. 14.

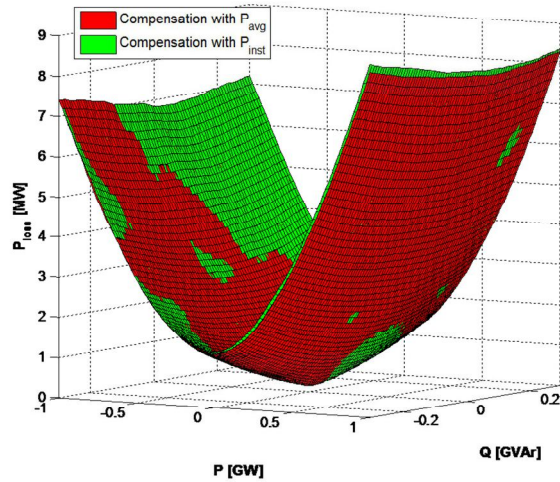


Figure 13. Comparisons between two types of power compensation in the energy-based control.

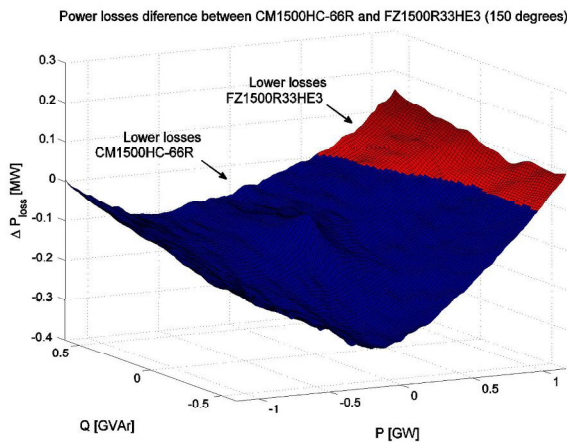


Figure 14. Comparison between the module Mitsubishi CM1500HC-66R and Infineon FZ1500R33HE3.

## VI. CONCLUSIONS

A complete numerical losses estimation method for the MMC is proposed. The losses are calculated for different operating points with high order approximation for the semiconductors characteristics instead of linear ones as it is typically done in the bibliography. Results have shown that using linear approximations drives to a considerable losses overestimation. The study of the passive losses reveals that they are in the same order of magnitude as the switching losses. In terms of computing time, this method is slightly slower than the existent analytic methods, but a complete simulation of a detailed MMC model can take tens of minutes.

Combining the average model and simulating only one arm the computation time is five times faster. The simulation time for each operating point is 1.5min with a processor Intel Xeon E5507 (2.27 GHz) and 6 GB RAM. The simulation of a complete P-Q range with a high number of operating points can be easily done with a standard computer.

## REFERENCES

- [1] A. Lesnicar and R. Marquardt, "An innovative modular multilevel converter topology suitable for a wide power range," in *Power Tech Conference Proceedings, 2003 IEEE Bologna*, vol. 3, June 2003, pp. 6 pp. Vol.3-.
- [2] C. Oates and C. Davidson, "A comparison of two methods of estimating losses in the modular multi-level converter," in *Power Electronics and Applications (EPE 2011), Proceedings of the 2011-14th European Conference on*, Aug 2011, pp. 1-10.
- [3] S. Samimi, F. Gruson, P. Delarue, and X. Guillaud, "Synthesis of different types of energy based controllers for a modular multilevel converter integrated in an hvdc link," in *AC and DC Power Transmission, 2015. ACDC. 14th IET International Conference on*.
- [4] H. Saad, X. Guillaud, J. Mahseredjian, S. Denetiere, and S. Nguafeu, "Mmc capacitor voltage decoupling and balancing controls," *Power Delivery, IEEE Transactions on*, vol. PP, no. 99, pp. 1-1, 2014.
- [5] S. Debnath, J. Qin, B. Bahrani, M. Saedifard, and P. Barbosa, "Operation, control, and applications of the modular multilevel converter: A review," *Power Electronics, IEEE Transactions on*, vol. 30, no. 1, pp. 37-53, Jan 2015.
- [6] S. Allebrod, R. Hamerski, and R. Marquardt, "New transformerless, scalable modular multilevel converters for hvdc-transmission," in *Power Electronics Specialists Conference, 2008. PESC 2008. IEEE, 2008*.
- [7] M. Zygmanski, B. Grzesik, M. Fulczyk, and R. Nalepa, "Analytical and numerical power loss analysis in modular multilevel converter," in *Industrial Electronics Society, IECON 2013 - 39th Annual Conference of the IEEE*, Nov 2013, pp. 465-470.
- [8] Q. Tu and Z. Xu, "Power losses evaluation for modular multilevel converter with junction temperature feedback," in *Power and Energy Society General Meeting, 2011 IEEE*, July 2011, pp. 1-7.
- [9] J. Peralta, H. Saad, S. Denetiere, J. Mahseredjian, and S. Nguafeu, "Detailed and averaged models for a 401-level mmc-hvdc system," in *Power and Energy Society General Meeting (PES), 2013 IEEE*, July 2013, pp. 1-1.
- [10] Mitsubishi HVIGBT modules, CM1500HC-66R, product specification sheet, Mar. 2009.
- [11] P. Jones and C. Davidson, "Calculation of power losses for mmc-based vsc hvdc stations," in *Power Electronics and Applications (EPE), 2013 15th European Conference on*, 2013, conference Location : Lille.
- [12] P. Delarue, F. Gruson, and X. Guillaud, "Energetic macroscopic representation and inversion based control of a modular multilevel converter," in *Power Electronics and Applications (EPE), 2013 15th European Conference on*, Sept 2013, pp. 1-10.
- [13] Q. Tu and Z. Xu, "Impact of sampling frequency on harmonic distortion for modular multilevel converter," *Power Delivery, IEEE Transactions on*, vol. 26, no. 1, pp. 298-306, Jan 2011.
- [14] F. Gruson, F. Colas, P. Delarue, J. Freytes, X. Guillaud and S. Samimi, "Impact of different control algorithms on Modular Multilevel Converters electrical waveforms and losses," unpublished, presented at the *19th European Conference on Power Electronics and Applications (EPE 2015)*, Sept. 2015, conference location: Geneva.
- [15] Infineon IGBT-inverter, FZ1500R33HE3 product specification sheet, Jul. 2010.